The Journal of Supercritical Fluids

Nanoparticle formation of PVP/astaxanthin inclusion complex by solution-enhanced dispersion by supercritical fluids (SEDS): Effect of PVP and astaxanthin *Z*-isomer content

Kahori Kaga[a], Masaki Honda[b,*], Tomoki Adachi[c], Masatoshi Honjo[c], Wahyudiono[a], Hideki Kanda[a] and Motonobu Goto[a,*]

[a] *Department of Materials Process Engineering, Nagoya University, Furo-cho, Chikusa-ku, Nagoya 464-8603, Japan*

[b] *Graduate School of Bioagricultural Sciences, Nagoya University, Furo-cho, Chikusa-ku, Nagoya 464-8601, Japan*

[c] *Research Institute, FANCL Corporation, Kamishinano, Totsuka-ku, Yokohama 244–0806, Japan*

*Corresponding author.

E-mail address: honda@agr.nagoya-u.ac.jp (M. Honda)

E-mail address: goto.motonobu@material.nagoya-u.ac.jp (M. Goto)

Abstract

The effects of operating conditions and *Z*-isomer content of astaxanthin on coprecipitate formation of polyvinylpyrrolidone (PVP) and astaxanthin by solution-enhanced dispersion by supercritical fluids (SEDS) process were investigated. Using this process, nano-sized (100–200 nm) and water-soluble PVP/astaxanthin inclusion complex was successfully prepared. As the operating pressure increased from 8 to 15 MPa at a constant temperature, astaxanthin content in the coprecipitates decreased, and increasing the operating temperature from 40 to 60 °C at a constant pressure, the particle size and the astaxanthin content increased. Increasing the PVP ratio for astaxanthin in the range of 5:1 to 20:1, the particle size decreased and when 10:1 of the ratio, the astaxanthin content in the coprecipitates was the highest (60 °C, 10 MPa). Additionally, as the *Z*-isomer content of astaxanthin increased, the astaxanthin content decreased slightly. However, the coprecipitates rich in astaxanthin *Z*-isomers, which have higher bioavailability and antioxidant capacity, were obtained.

Keywords: Carotenoid, Polyvinylpyrrolidone, Coprecipitation, Supercritical anti-solvent, *E*/*Z* isomerization

1. Introduction

Carotenoids are the most common fat-soluble pigments that give yellow, orange, and red colors to plants and animals, and more than 750 different types have been characterized until now [1]. The daily consumption of carotenoids-rich foods would be beneficial for human health because of the prevention effect of various diseases such as certain cancers and atherosclerosis as well as high antioxidant capacity [2−4]. Moreover, carotenoids are attracting attention as safe natural colorants in food products and as an alternative to synthetic colorants which are not well accepted by consumers.

Astaxanthin is a keto carotenoid containing 13 conjugated double bonds, and is found abundantly in the marine world of algae and aquatic animals with a dark-red color [5]. As with other carotenoids, astaxanthin has high antioxidant capacity and ability to prevent and treat various diseases such as cancers, chronic inflammatory diseases, and cardiovascular diseases [4−6]. For these reasons, there is a strong interest in using astaxanthin as functional and natural colorant in food industry. However, the poor water solubility of astaxanthin has made its use problematic for food formulations and the favorable effects of astaxanthin are limited. Furthermore, the low solubility in water of functional lipid bioactive compounds would be prone to reduce the bioavailability [7,8]. Therefore, it is very important to improve their dispersibility in water by emulsification for food industry and increment their bioavailability. When preparing carotenoids dispersions, nano-level particle size is preferable due to the high dispersibility and bioavailability [9,10].

Polyvinylpyrrolidone (PVP; Fig. 1A) is a hydrophilic carrier and has acquired broad applications in food and pharmaceutical industries [11]. It has the effect of suppressing crystal growth of compounds with high crystallinity [12] and can improve

the solubility of poorly water-soluble compounds [13]. In addition, since PVP contains a proton acceptor, it is able to form H-bonds with a proton donator group [14,15]. The H-bonding enhances the extent of interaction between the proton donator and PVP so that the matrix can exist stably. Therefore, PVP is considered to be a suitable carrier for carotenoids having high hydrophobicity and crystallinity. Moreover, its use is considered to be more suitable for xanthophylls such as astaxanthin and lutein, which contain proton donator groups, e.g. hydroxyl group. There is limited evidence that water dispersibility of carotenoids such as β-carotene and lutein was improved using PVP [11,14,15].

In many studies, the formation of carotenoids-containing nanodispersions is conducted by emulsification-evaporation, emulsification-diffusion, and solvent-displacement techniques [16]. However, these techniques use toxic organic solvents to dissolve carotenoids in oil phase and have a concern that the solvents remain in the obtained emulsions [8,16,17]. Thus, in recent years, the formation of nanodispersions utilizing supercritical CO_2 (SC-CO_2), which is non-toxic and easily separated from the products, has been extensively examined. The supercritical anti-solvent (SAS) process is one of the micronization methods which can be applied for preparing fine particles from various materials such as pharmaceuticals, coloring matters, biopolymers [11,18,19]. In this study, the coprecipitation of PVP and astaxanthin was carried out using the method of solution-enhanced dispersion by supercritical fluids (SEDS), which is a modified version of the SAS process [20,21]. In this process, the solution and SC-CO_2 are sprayed into a precipitator by a coaxial nozzle. In a typical SEDS process, an anti-solvent fluid (SC-CO_2) and a solution containing compounds to be processed are injected via the nozzle into a precipitation vessel continuously, and particles are formed

when supersaturation of the compounds is achieved. Additionally, the particle size is easily controlled by the preparation conditions such as pressure and temperature.

Although there are limited number of literatures, water dispersibility of carotenoids was improved by coprecipitate formation with several hydrophilic carriers using SC-CO_2 as the anti-solvent [11,21−25]. For example, Prosapio et al. [11] have reported that β-carotene-containing nanoparticles with high water dispersibility could be obtained by coprecipitation of the carotenoid and PVP using SAS process. Moreover, an example of improving the water dispersibility of lycopene using β-cyclodextrin as a carrier by the solution-enhanced dispersion by SEDS process has also been reported by Nerome et al. [21]. However, to the best of our knowledge, there have been no reports about coprecipitation of astaxanthin and PVP using SC-CO_2 as an anti-solvent, and the previous literatures on coprecipitation of carotenoids and hydrophilic carriers using SAS or SEDS method evaluated only particle morphology, particle size, and dissolution efficiency in water of obtained coprecipitates, while carotenoid content and encapsulation efficiency of astaxanthin in the coprecipitates was not assessed [11,21−25]. Furthermore, the effect of *Z*-isomerization pre-treatment of (all-*E*)-astaxanthin was also investigated in this study (Fig. 1B−D). Since *Z*-isomers of carotenoids have higher solubility and lower crystallinity than the all-*E* isomers [26−29], the mean diameter, particle morphology, and astaxanthin content of the obtained particles would be affected. In fact, Kodama et al. [20] have reported that when lycopene was micronized by SEDS process, as the *Z*-isomer content of lycopene increased, the size of obtained particle became smaller. Additionally, since *Z*-isomers of astaxanthin have higher bioavailability [30] and antioxidant capacity [31,32] than the all-*E*-isomer, to obtain coprecipitates of PVP and *Z*-isomer-rich astaxanthin would result

in the improvement of the functional value. Therefore, the aim of the study is to clarify the effect of operating conditions and *Z*-isomer content of astaxanthin on coprecipitate formation of astaxanthin and PVP using SEDS process.

2. Materials and methods

2.1. Chemicals

High purity (all-*E*)-astaxanthin (synthetic) and PVP (average molecular weight 10,000) were obtained by Sigma-Aldrich Co. Ltd. (Dorset, United Kingdom). High-performance liquid chromatography (HPLC)-grade methanol, acetonitrile, and dichloromethane (CH_2Cl_2) were purchased from Kanto Chemical Co., Inc. (Tokyo, Japan), and HPLC-grade acetone and analytical grade ethanol were purchased from Wako Pure Chemical Industries, Ltd. (Osaka, Japan).

2.2. Preparation of astaxanthin Z-isomers

Astaxanthin that contains a large amount of *Z*-isomers was prepared by the thermal isomerization and filtering technique from (all-*E*)-astaxanthin described previously [20,33,34]. Briefly, (all-*E*)-astaxanthin was dissolved in CH_2Cl_2 at a concentration of 1 mg/mL and heated at 80 °C for 3 h. Then, the thermally treated astaxanthin solution was evaporated to dry under reduced pressure at 40 °C and the residue (ca. 50 mg) was suspended in 10 mL of hexane. The insoluble substances, mostly consisting of (all-*E*)-astaxanthin, were removed using a 0.2-μm polytetrafluoroethylene (PTFE) membrane filter (DISMIC-25HP, Advantec, Tokyo), and hexane was removed under reduced pressure at 40 °C. In this study, (all-*E*)-astaxanthin, thermally *Z*-isomerized astaxanthin, and the filtered astaxanthin after thermal treatment were used as raw materials for

coprecipitate formation using the SEDS process.

2.3. Equipment and procedure

A schematic diagram of the SEDS micronization is shown in Fig. 2. The apparatus includes a chiller (CCA-1111, Tokyo Rikakikai Co., Ltd., Tokyo), two high-pressure pumps, one for CO_2 (PU–2086, Jasco Co., Tokyo) and the other for the astaxanthin and PVP solution (LC–20AT, Shimadzu Co., Ltd., Kyoto, Japan), a heating chamber (EI-700B, As One Co., Osaka, Japan), a coaxial nozzle with inside diameter 0.5 mm (SUS-316), a filter for collecting particles (500 nm SUS-316) placed inside a Swagelok filter housing, a back-pressure regulator (BPR; Akico Co., Ltd., Tokyo), and a wet gas meter (Shinagawa Co., Ltd., Tokyo). Liquid CO_2 flowing from the CO_2 cylinder was compressed and controlled with the high-pressure pump which was cooled with a chiller to keep CO_2 in a liquid state. In the heating chamber, CO_2 was transformed into a supercritical state by heating.

The coprecipitation of PVP and astaxanthin using the above apparatus was performed according to the following procedures [11,20,21]. SC-CO_2 was flowed to the filter at a flow rate of 15 mL/min until the desired pressure and temperature conditions were reached. The astaxanthin and PVP solution (acetone/ethanol, 19:1, v/v) were then injected at 0.1 mL/min for 1 h. At the end of each experiment, SC-CO_2 was pumped to flow continuously for 30 min to eliminate the remaining organic solvent from the particles. Finally, the particles were collected from the membrane filter after depressurization. The experiment was carried out at pressures of 8–15 MPa and temperatures of 40–60 °C. The contents of PVP and astaxanthin in acetone/ethanol solution were 0.73–2.94 and 0.14 mg/mL, respectively: PVP/astaxanthin ratio:

approximately 5:1–20:1, and the range of *Z*-isomer contents of astaxanthin were 0–66.2%. Table 1 shows the summary of experimental conditions with the results of mean diameter and astaxanthin content of the coprecipitates obtained.

2.4. SEM analysis

The shape and surface characteristics of the PVP/astaxanthin coprecipitates as well as PVP and (all-*E*)-astaxanthin, which were raw materials, were observed by scanning electron microscopy (SEM; JSM-6390LV JEOL, Tokyo, Japan). The samples were sputter-coated with gold in a high-vacuum evaporator and examined using SEM at 15 kV [20]. Particle size and size distributions were measured using Image J software for at least 250 particles collected at each experiment [20,21].

2.5. FT-IR analysis

The characteristics of chemical structures of the PVP/astaxanthin coprecipitates as well as PVP and (all-*E*)-astaxanthin, which were raw materials, were analyzed by a Spectrum One Fourier transform infrared (FT-IR) spectrophotometer (Perkin-Elmer Ltd., Buckinghamshire, United Kingdom). The samples were placed directly in the diffuse reflectance attachment sample holder. Pre-flattening of the sample in a diamond cell was necessary prior to mounting. The spectra were measured in ATR (attenuated total reflectance) mode (golden single reflection ATR system, P/N 10500 series, Specac) at 4 cm^{-1} resolution. The scanning wavenumber ranged from 4000 to 500 cm^{-1} [35].

2.6. Powder XRD analysis

Powder X-ray diffraction (XRD) measurements of PVP/astaxanthin coprecipitates as

well as intact PVP and (all-*E*)-astaxanthin were carried out on a Rigaku FR-E X-ray diffractometer. Cu Kα radiation (λ = 1.542 Å) was used with a beam size of approximately 300 μm × 300 μm, with a camera length of 70 mm. The powder sample was placed in a capillary tube (⌀1.0 mm) and was irradiated with the X-ray beam without further adjustments [20].

2.7. Encapsulated astaxanthin content

Content of encapsulated astaxanthin in PVP was determined by measurement of the absorbance of the prepared coprecipitates at 480 nm using an UV/VIS spectrophotometer (V-550, JASCO Co., Tokyo, Japan). Before the measurement, the obtained coprecipitates were accurately weighed using an analytical balance (±0.1 μg, XP2UV, Mettler-Toledo, Inc., Columbus, OH, USA) and diluted with distilled water until the absorbance at the wavelength (480 nm) was between 0.3 and 1.0 absorbance units. The absorbance determined with this method is proportional to the amount of astaxanthin dispersed in solution. However, since the particles of crystalline astaxanthin are not stabilized in the suspension, they do not contribute to the absorbance determined with this method [36,37].

2.7. HPLC analysis

To determine *Z*-isomer content of astaxanthin, reversed-phase HPLC analysis with a C_{18} column (STR-ODS II, 250 × 4.6 mm i.d., Shinwa Chemical Industries Ltd., Kyoto, Japan) was carried out according to the method described previously [33]. The mobile phase consisted of methanol/acetonitrile/CH_2Cl_2/water (85:5.5:5:4.5, v/v), and the flow rate and column temperature were set at 1 mL/min and 30 °C, respectively. The

quantification of *Z*-isomers of astaxanthin was carried out by peak area integration at 480 nm by a photodiode array detector (SPD-M10A, Shimadzu, Kyoto, Japan). Astaxanthin isomer peaks were identified according to HPLC retention times, visible spectral data, and relative intensities of the *Z*-peak at approximately 370 nm to the absorption maximum of the isomer (% D_B/D_{II}), as described previously [33,38,39]. When determining the *Z*-isomer content in the coprecipitates, before the HPLC analysis, astaxanthin isomers were extracted by ethanol/hexane (2:3, v/v) according to the method of Yuan et al. (2008) [40]. The extracted astaxanthin was dissolve in the same solution as the mobile phase and filtered through a 0.2-μm PTFE membrane filter. The astaxanthin *Z*-isomer content (%) was estimated as the amount of total *Z*-isomers to the amount of total astaxanthin isomers including the all-*E*-isomers.

3. Results and discussion

3.1. General characteristics of PVP/astaxanthin coprecipitates

The characteristics of coprecipitates of PVP and (all-*E*)-astaxanthin obtained by SEDS process were assessed. The evaluation was conducted for the coprecipitates obtained at pressure of 10 MPa and temperature of 60 °C for 1 h, and 20:1 of PVP/(all-*E*)-astaxanthin ratio.

3.1.1. Particle morphology and size

SEM images of the PVP/(all-*E*)-astaxanthin coprecipitates as well as intact PVP and (all-*E*)-astaxanthin are shown in Fig. 3. Before the SEDS process, PVP was white powder (Fig. S1A) and approximately 30-μm-diameter spherical particles (Fig. 3A), and (all-*E*)-astaxanthin was dark reddish-black powder (Fig. S1B) [5] and approximately 3-

μm-diameter flake-shaped crystals (Fig. 3B). On the other hand, after the SEDS process, the obtained coprecipitates was bright-red powder (Fig. S1C) and approximately 200-nm-diameter spherical particles (Fig. 3C). Prosapio et al. [11] and Nerome et al. [21] have also reported that when carotenoids such as β-carotene and lycopene were treated with SAS or SEDS process together with hydrophilic carriers such as PVP and β-cyclodextrin, nano-level spherical particles were obtained.

3.1.2. Solubility in water

The solubility in water of the obtained coprecipitates were investigated using the UV/VIS spectrophotometer. The evaluations were conducted for PVP, (all-*E*)-astaxanthin, and the coprecipitates which were dissolved in water to be the same concentration (wt%). Fig. 4A shows the absorption wavelengths of the samples in water. The coprecipitate had the absorbance in the range of 400 to 600 nm, which was astaxanthin-specific absorbance [33,38,39]. On the other hand, water-dissolved (all-*E*)-astaxanthin had no absorbance. The compound-specific absorbance can be observed when the compound disperses in the solution [36,37]. Therefore, this results indicated that water-soluble PVP/astaxanthin inclusion complex had been successfully formed using the SEDS process. Moreover, since the absorbance determined by UV/VIS spectrophotometer is proportional to the amount of astaxanthin dispersed in solution and only astaxanthin encapsulated by PVP was detected [36,37], the quantification of astaxanthin was conducted by using the method in this study.

3.1.3. FT-IR analysis

Fig. 4B shows the FT-IR spectra of PVP/astaxanthin coprecipitates as well as intact

PVP and (all-*E*)-astaxanthin. As for PVP and (all-*E*)-astaxanthin, the same spectra patterns were observed in previous studies [41,42]. The spectrum of the coprecipitates showed the same pattern with that of intact PVP: although IR spectrum of pure astaxanthin showed the characteristics of very strong absorption band at 1547 cm^{-1} for stretching vibration of C=C in the hexatomic ring and 974 cm^{-1} for C−H stretching vibration in C, C conjugate system, those absorption band were disappeared. This is probably because (all-*E*)-astaxanthin was encapsulated in PVP. In fact, a number of studies have reported that when compounds were encapsulated in carriers including PVP, the FT-IR spectra shows the same pattern as those [42,43].

3.1.4. Powder XRD analysis

Fig. 4C shows the powder XRD patterns of PVP/astaxanthin coprecipitates as well as intact PVP and (all-*E*)-astaxanthin. As for PVP and (all-*E*)-astaxanthin, the same spectra patterns as previous studies were observed [44−46]. On the other hand, as for the coprecipitates, the spectra peculiar to (all-*E*)-astaxanthin disappeared completely and showed PVP-like XRD patterns: two broad peaks were observed at a diffraction angle 2θ value of 10–25°. This result has observed in previous studies which prepared coprecipitation by supercritical antisolvent process using PVP as a carrier [45,46], and it indicated that (all-*E*)-astaxanthin formed complexes with PVP.

3.2. Effect of pressure

3.2.1. Particle morphology and size

The effect of operating pressure on particle morphology and size of obtained coprecipitates was investigated by SEM analysis. The obtained particles were spherical

and there were no significant differences in particle morphology at any pressure (Fig. S2). The mean particle size was approximately 150 nm at 8 and 10 MPa, while when processing at 15 MPa, the mean particle size increased slightly (175 nm) and the particle size distribution expanded (Table 1, Fig. 5A). Generally, increasing the operating pressure, the obtained particle size become smaller due to increase of anti-solvent (SC-CO_2) density: fast mixing and mass transfer at higher densities lead to smaller particles [46]. Several studies using PVP under SAS process has been also reported that as the operating pressure increased, the particle size decreases [11,45,47]. However, as the anti-solvent density increases, the diffusivity of the organic solvent decreases and the mass transfer and mixing would slow down. That may result in increment of the particle size [46,48]. As an example, Uzun et al. [44] reported that when preparing PVP/cefuroxime axetil inclusion complex by SAS process from the methanol solution, the obtained particle size increased by increasing the operating pressure.

3.2.2. Encapsulated astaxanthin content

The encapsulated astaxanthin content corresponding to operating pressure was determined using an UV/VIS spectrophotometer. When the coprecipitation of PVP and (all-*E*)-astaxanthin by SEDS process was performed at temperature of 40 °C and pressures of 8, 10, 15 MPa, the astaxanthin content of obtained particles were 0.51, 0.33, and 0.07%, respectively. It seemed that the lower the pressure resulted to the higher the astaxanthin content in the coprecipitation. It has been known that operating pressure may give effects on the CO_2 density in supercritical condition and the viscosity of solution. It also affected to the mass transfer of solutes, in particular, organic solvents

having low molecular weight, in SC-CO_2 during precipitation process. Namely, as the operating pressure reduced, the mass transfer of the organic solvents increased and they immediately diffused into SC-CO_2. As the result, PVP and astaxanthin might rapidly form complexes and thus the recovery of astaxanthin increased [49,50]. Although the astaxanthin content in the particles was highest at pressure of 8 MPa, here, the subsequent experiments were performed at pressure of 10 MPa. Martin et al. [51] conducted experiments for coprecipitation of carotenoids and bio-polymers with the supercritical anti-solvent process. They reported that the carotenoid particles were covered partially by polymer as a coprecipitator when the experiments were performed at pressure of 8 MPa. Hence, in this work, the operating pressure of experiments were fixed at 10 MPa.

On the other hand, since PVP/astaxanthin ratio in the starting solution was 20:1, if all PVP and astaxanthin precipitated by this process, astaxanthin content should be approximately 5%. However, the content was significantly lower than 5%. This is probably because astaxanthin has much higher solubility in SC-CO_2 than PVP (about 100 times higher) [52,53], i.e. since a large amount of astaxanthin was the dissolution state in SC-CO_2, it passed through the particulate collection filter and/or astaxanthin was extracted from coprecipitates in the 30 min of organic solvent removal process.

3.3. Effect of temperature

3.3.1. Particle morphology and size

The influence of operating temperature on particle morphology and size of PVP/astaxanthin coprecipitates was evaluated. The temperatures were varied between 40−60 °C. All the obtained particles were spherical, and there was no significant

difference in particle morphology at any temperatures at operating pressure of 10 MPa (Fig. S3). On the other hand, increasing the operating temperature, the particle size increased and particle size distribution expanded (Table. 1, Fig. 5B). Generally, in SAS precipitation, as the temperature increases, since the density of SC-CO_2 decreases, the mass transfer rate decreases. In accordance with that, the supersaturation ratio decreased and larger particles were formed [46]. This tendency was also observed in other studies of SAS coprecipitation using PVP as a carrier [45,47].

3.3.2. Encapsulated astaxanthin content

When the SEDS process was performed at temperatures of 40, 50, 60 °C and pressure of 10 MPa, the astaxanthin content in the obtained particles were 0.33, 0.49, and 1.43%, respectively. It showed that the higher operating temperature resulted in the higher astaxanthin content of the obtained coprecipitates. As with operating pressure, the temperature also gave effects on the CO_2 density in supercritical condition and the viscosity of solution, and consequently, it affected to the mass transfer of the solutes, in particular organic solvents. Raising the operating temperature, the mass transfer of organic solvents increased, they immediately diffused into SC-CO_2, and then PVP and astaxanthin might rapidly form complexes. As the result, it is considered that the recovery of astaxanthin increased [49,50]. Moreover, the nucleation rate of solute also increased with increasing operating temperature at a constant operating pressure.

3.4. Effect of PVP/astaxanthin ratio

3.4.1. Particle morphology and size

The obtained particles were spherical, and there was no significant difference in

particle morphology at any PVP/astaxanthin ratio at pressure of 10 MPa and temperature of 60 °C (Fig. S4). On the other hand, as the PVP ratio decreased, the particle size decreased and particle size distribution was narrow (Fig. 6A). This tendency was also observed in the other studies of SAS coprecipitation using PVP as a carrier [45,48]. It is considered that the supersaturation ratio of PVP/astaxanthin coprecipitates in SC-CO_2 increased by decreasing PVP ratio so that the particle size decreased.

3.4.2. Encapsulated astaxanthin content

In the case of processing in the PVP/astaxanthin ratio of 20:1, 10:1, and 5:1 under the operating conditions at temperature of 60 °C and pressure of 10 MPa, the astaxanthin content of the coprecipitates were 1.43, 3.91, and 3.90%, respectively. It showed that when the PVP/astaxanthin ratio as a feed solution was 10:1, the highest of astaxanthin content in particles products was found. Regarding to the active compounds encapsulation, essentially, there are two tendencies: the active compounds can be coated by a thin layer of polymer or the active compounds and polymer can be precipitated to produce fine particles with the active compounds impregnated into polymeric particles [50]. Generally, the active compounds coated by polymer is better when the polymer concentration is increased and a shift in the polymer concentration may lead to change morphology of particles. However, as shown above, there was no significant difference in particle morphology at any PVP/astaxanthin ratio between 5:1 and 10:1. Additionally, when the ratio was 10:1, the amount of coprecipitates obtained was approximately 1.3 times higher than 5:1 of the ratio. Based on the result, the subsequent experiments were performed in the PVP/astaxanthin ratio of 10:1, which has the highest

recovery of astaxanthin.

3.5. Effect of Z-isomer content of astaxanthin

3.5.1. Profile of astaxanthin isomers obtained by thermal isomerization and filtration

Ample studies have demonstrated that (all-*E*)-carotenoids easily isomerized to the *Z*-isomers in organic solvents by heating [20,26,33]. (all-*E*)-Astaxanthin was also isomerized to the *Z*-isomers by heating at temperature of 80 °C in CH_2Cl_2 for 3 h in this study. After the heating, the total *Z*-isomer content reached 39.4%. Furthermore, after the thermally treated astaxanthin was dissolved in hexane and filtered by a 0.2-μm PTFE membrane filter, the total *Z*-isomer content further increased to 66.2%. This was because *Z*-isomers of carotenoids were more soluble in solvents than the (all-*E*)-isomers [20,26−28], i.e. since (all-*E*)-astaxanthin was low solubility in hexane, the isomer was removed by the filtration. The reversed-phase HPLC charts of (all-*E*)-astaxanthin and the thermally *Z*-isomerized and filtered samples are shown in Fig. 7. Peaks in Fig. 7 were tentatively identified by those absorption spectra and relative intensities of the *Z*-peak (% D_B/D_{II}) referring to literatures (Fig. S5 and Table S1) [33,38,39]. As with previous studies of thermal isomerization of (all-*E*)-astaxanthin in organic solvents [33,38], (9*Z*)- and (13*Z*)-astaxanthin emerged. The coprecipitation of PVP and astaxanthin containing 39.4% and 66.2% of the *Z*-isomers was performed by SEDS process.

3.5.2. Particle morphology and size

The effect of *Z*-isomer content of astaxanthin on particle morphology and size of obtained coprecipitates was investigated by SEM analysis. The obtained particles were

spherical, and when using astaxanthin having the highest *Z*-isomer content (66.2%), a small number of agglomerated particles were observed (Fig. S6). Thus, although the mean particle size did not have a big difference by the *Z*-isomer content, when 66.2% of *Z*-isomer content astaxanthin was used as the raw material, the particle size distribution expanded slightly (Fig. 6B). The physical properties such as solubility and crystallinity of carotenoids significantly changed by the *E*/*Z* isomerization [26−29]. Those changes would affect the particle size and particle size distribution of the coprecipitates with PVP. In fact, Prosapio et al. [54] showed that components difference affected the particle size of coprecipitates with PVP obtained by SAS precipitation.

3.5.3. Encapsulated astaxanthin concentration

When using (all-*E*)-astaxanthin and astaxanthin of which the *Z*-isomer contents were 39.4% and 66.2% as raw materials of the PVP/astaxanthin coprecipitation by SEDS process at pressure of 10 MPa and temperature of 60 °C, the astaxanthin content of obtained particles were 3.91, 3.78, and 3.56%, respectively, and the total *Z*-isomer contents were 8.2, 40.2, 58.7% (Fig. S7), respectively. Although it was a slight change, the higher the *Z*-isomer content in the raw material, the lower the astaxanthin content in the obtained coprecipitates. *Z*-Isomers of carotenoids are more soluble in solvents including SC-CO_2 than the all-*E*-isomer [26−28]. Therefore, it is considered that since the supersaturation ratio of astaxanthin in SC-CO_2 increased by the *Z*-isomerization pre-treatment, the efficiency of coprecipitation formation decreased, or in the solvent removal process after coprecipitation formation, several *Z*-isomers including in the coprecipitates was extracted due to the high solubility in SC-CO_2. However, by using PVP as a carrier, most of astaxanthin *Z*-isomers were successfully included in it and

formed nanocoprecipitates. Our previous study [20] have attempted to obtain *Z*-isomer-rich lycopene particles from lycopene containing a large amount of the *Z*-isomer by SEDS precipitation, though since the *Z*-isomers had high solubility in SC-CO_2, the particles could not be formed. As with other carotenoids such as lycopene [55−57], *Z*-isomers of astaxanthin have higher bioavailability [30] and antioxidant capacity [31,32] than the all-*E*-isomer. Thus, although the encapsulation efficiency of astaxanthin is slightly lowered, the use of *Z*-isomer-rich astaxanthin as the raw material for PVP/astaxanthin coprecipitation by SEDS process would result in improvement the functionality of the coprecipitates.

4. Conclusion

Water-soluble PVP/astaxanthin nanocoprecipitates were successfully prepared by SEDS precipitation. It was found that the operating pressure, temperature, PVP/astaxanthin ratio, and *Z*-isomer content of astaxanthin affect the particle size and/or astaxanthin content in the coprecipitates: increasing the pressure in the range of 8−15 MPa, the astaxanthin content decreased; increasing the temperature in the range of 40−60 °C, the particle size and the astaxanthin content increased; increasing the PVP ratio for astaxanthin in the range of 5:1−20:1 the particle size increased and when 10:1 of the ratio, the astaxanthin content was the highest; increasing the *Z*-isomer content of astaxanthin in the range of 0−66.2%, the astaxanthin content decreased. Therefore, it is considered that fine and high astaxanthin content water-soluble particles can be obtained by optimizing these parameters. Furthermore, it is known that since the *Z*-isomers of carotenoids have high solubility in solvents including SC-CO_2, preparation of the fine particles by anti-solvent processing is difficult. However, by the

coprecipitation with PVP, the fine particles rich in *Z*-isomers of astaxanthin successfully obtained. As the *Z*-isomers of astaxanthin have higher bioavailability and antioxidant capacity than the all-*E*-isomer, the use of *Z*-isomers of astaxanthin as the raw material of PVP/astaxanthin coprecipitation would improve the functionality of the coprecipitate.

References

[1] T. Maoka, T. Carotenoids in marine animals. Mar. Drugs 9 (2011) 278−293.

[2] N.I. Krinsky, E.J. Johnson, Carotenoid actions and their relation to health and disease. Mol. Asp. Med. 26 (2005) 459−516.

[3] X.R. Xu, Z.Y. Zou, Y.M. Huang, X. Xiao, L. Ma, X.M. Lin, Serum carotenoids in relation to risk factors for development of atherosclerosis. Clin. Biochem. 45 (2012) 1357−1361.

[4] A. Ouchi, K. Aizawa, Y. Iwasaki, T. Inakuma, J. Terao, S. Nagaoka, K. Mukai, Kinetic study of the quenching reaction of singlet oxygen by carotenoids and food extracts in solution. Development of a singlet oxygen absorption capacity (SOAC) assay method, J. Agric. Food Chem. 58 (2010) 9967−9978.

[5] J. Dhankhar, S.S. Kadian, A. Sharma, Astaxanthin: A potential carotenoid. Int. J. Pharm. Sci. Res. 3 (2012) 1246−1259.

[6] G. Hussein, U. Sankawa, H. Goto, K. Matsumoto, H. Watanabe, H. Astaxanthin, a carotenoid with potential in human health and nutrition. J. Nat. Prod. 69 (2006) 443−449.

[7] A. Spernath, A. Aserin, Microemulsions as carriers for drugs and nutraceuticals. Adv. Colloid Interface Sci. 128 (2006) 47–64.

[8] N. Anarjan, C.P. Tan, Effects of selected polysorbate and sucrose ester emulsifiers

on the physicochemical properties of astaxanthin nanodispersions. Molecules 18 (2013) 768–777.

[9] L. Salvia-Trujillo, C. Qian, O. Martín-Belloso, D.J. McClements, Influence of particle size on lipid digestion and β-carotene bioaccessibility in emulsions and nanoemulsions. Food Chem. 141 (2013) 1472–1480.

[10] R. Vishwanathan, T.A. Wilson, R.J. Nicolosi, Bioavailability of a nanoemulsion of lutein is greater than a lutein supplement. Nano Biomed. Eng. 1 (2009) 38–49.

[11] V. Prosapio, E. Reverchon, I. De Marco, Coprecipitation of polyvinylpyrrolidone/β-carotene by supercritical antisolvent processing. Ind. Eng. Chem. Res. 54 (2015) 11568–11575.

[12] G.A. Ledet, R.A. Graves, E.Y. Glotser, T.K. Mandal, L.A. Bostanian, Preparation and in vitro evaluation of hydrophilic fenretinide nanoparticles. Int. J. Pharm. 479 (2015) 329–337.

[13] M.P. Oth, A.J. Moes, Enhanced in vitro release of indomethacin from non-aqueous suspensions using indomethacin-polyvinylpyrrolidone coprecipitate. Int. J. Pharm. 24 (1985) 275–286.

[14] C. Zhao, H. Cheng, P. Jiang, Y. Yao, J. Han, Preparation of lutein-loaded particles for improving solubility and stability by polyvinylpyrrolidone (PVP) as an emulsion-stabilizer. Food Chem. 156 (2014) 123–128.

[15] W. Liu, J. Wang, M. Li, W. Tang, J. Han, Molecular mechanism of the protective effect of monomer polyvinylpyrrolidone on antioxidants–experimental and computational studies. SAR QSAR Environ. Res. 27 (2016) 1015–1027.

[16] D. Horn, J. Rieger, Organic nanoparticles in the aqueous phase—theory, experiment, and use. Angew. Chem. Int. Ed. 40 (2001) 4330–4361.

[17] C.P. Tan, M. Nakajima, β-Carotene nanodispersions: preparation, characterization and stability evaluation. Food Chem. 92 (2005) 661–671.

[18] I. De Marco, V. Prosapio, F. Cice, E. Reverchon, Use of solvent mixtures in supercritical antisolvent process to modify precipitates morphology: Cellulose acetate microparticles. J. Supercrit. Fluids 83 (2013) 153–160.

[19] Y. Wang, Y. Wang, J. Yang, R. Pfeffer, R., Dave, B. Michniak, The application of a supercritical antisolvent process for sustained drug delivery. Powder Technol. 164 (2006) 94–102.

[20] T. Kodama, M. Honda, R. Takemura, T. Fukaya, C. Uemori, H. Kanda, M. Goto, Effect of the *Z*-isomer content on nanoparticle production of lycopene using solution-enhanced dispersion by supercritical fluids (SEDS). J. Supercrit. Fluids 133 (2018) 291–296.

[21] H. Nerome, S. Machmudah, R. Fukuzato, T. Higashiura, Y.S. Youn, Y.W. Lee, M. Goto, Nanoparticle formation of lycopene/β-cyclodextrin inclusion complex using supercritical antisolvent precipitation, J. Supercrit. Fluids 83 (2013) 97–103.

[22] E. Franceschi, A.M. De Cesaro, M. Feiten, S.R.S Ferreira, C. Dariva, M.H. Kunita, A.F. Rubire, E.C. Muniz, M.L. Corazza, J.V. Oliveira, Precipitation of β-carotene and PHBV and co-precipitation from SEDS technique using supercritical CO_2. J. Supercrit. Fluids 47 (2008) 259–269.

[23] A. Martín, F. Mattea, L. Gutiérrez, F. Miguel, M.J. Cocero, Co-precipitation of carotenoids and bio-polymers with the supercritical anti-solvent process. J. Supercrit. Fluids 41 (2007) 138–147.

[24] F. Miguel, A. Martín, F. Mattea, M.J. Cocero, Precipitation of lutein and co-precipitation of lutein and poly-lactic acid with the supercritical anti-solvent process. Chem. Eng. Proc.: Proc. Intensif. 47 (2008) 1594–1602.

[25] W.L. Priamo, A.M. de Cezaro, S.R. Ferreira, J.V. Oliveira, Precipitation and encapsulation of β-carotene in PHBV using carbon dioxide as anti-solvent. J. Supercrit. Fluids 54 (2010) 103–109.

[26] K. Murakami, M. Honda, R. Takemura, T. Fukaya, M. Kubota, Wahyudiono, H. Kanda, M. Goto, The thermal *Z*-isomerization-induced change in solubility and physical properties of (all-*E*)-lycopene, Biochem. Biophys. Res. Commun. 491 (2017) 317–322.

[27] M. Honda, Y. Watanabe, K. Murakami, R. Takemura, T. Fukaya, Wahyudiono, H. Kanda, M. Goto, Thermal isomerization pre-treatment to improve lycopene extraction from tomato pulp, LWT-Food Sci. Technol. 86 (2017) 69–75.

[28] M. Honda, Y. Watanabe, K. Murakami, N.N. Hoang, H. Kanda, M. Goto, Enhanced lycopene extraction from gac (*Momordica cochinchinensis* Spreng.) by the *Z*-isomerization induced with microwave irradiation pre-treatment. Eur. J. Lipid Sci. Technol. 1700293 (2018) 1–8.

[29] J. Hempel, C.N. Schädle, S. Leptihn, R. Carle, R.M. Schweiggert, Structure related aggregation behavior of carotenoids and carotenoid esters. J. Photochem. Photobiol. A Chem. 317 (2016) 161–174.

[30] C. Yang, H. Zhang, R. Liu, H. Zhu, L. Zhang, R. Tsao, Bioaccessibility, cellular uptake, and transport of astaxanthin isomers and their antioxidative effects in human intestinal epithelial caco-2 cells. J. Agric. Food Chem. 65 (2017) 10223−10232.

[31] C. Yang, L. Zhang, H. Zhang, Q. Sun, R. Liu, J. Li, L. Wu, R. Tsao, Rapid and efficient conversion of all-*E*-astaxanthin to 9*Z*- and 13*Z*-isomers and assessment of their

stability and antioxidant activities. J. Agric. Food Chem. 65 (2017) 818−826.

[32] X. Liu, T. Osawa, *Cis* astaxanthin and especially 9-*cis* astaxanthin exhibits a higher antioxidant activity *in vitro* compared to the all-*trans* isomer. Biochem. Biophys. Res. Commun. 357 (2007) 187−193.

[33] J.P. Yuan, F. Chen, Isomerization of *trans*-astaxanthin to *cis*-isomers in organic solvents. J. Agric. food Chem. 47 (1999) 3656–3660.

[34] M. Honda, T. Kudo, T. Kuwa, T. Higashiura, T. Fukaya, Y Inoue, C. Kitamura, M. Takehara, Isolation and spectral characterization of thermally generated multi-*Z*-isomers of lycopene and the theoretically preferred pathway to di-*Z*-isomers. Biosci. Biotechnol. Biochem. 81 (2017) 365–371.

[35] S. Machmudah, Q.Y.A. Shiddiqi, A.D. Kharsma, Widiyastuti, Wahyudiono, H. Kanda, S. Winardi, M. Goto, Subcritical water extraction of xanthone from mangosteen (*Garcinia Mangostana Linn*) pericarp. J. Adv. Chem. Eng. 5 (2015) 1–6.

[36] A. Tachaprutinun, T. Udomsup, C. Luadthong, S. Wanichwecharungruang, Preventing the thermal degradation of astaxanthin through nanoencapsulation. Int. J. Pharm. 374 (2009) 119–124.

[37] E. de Paz, Á. Martín, E. Mateos, M.J. Cocero, Production of water-soluble β-carotene micellar formulations by novel emulsion techniques. Chem. Eng. Proc.: Proc. Intensif. 74 (2013) 90−96.

[38] L. Zhao, F. Chen, G. Zhao, Z, Wang, X. Liao, X. Hu, Isomerization of *trans*-astaxanthin induced by copper (II) ion in ethanol. J. Agric. food Chem. 53 (2005) 9620–9623.

[39] C. Yang, L. Zhang, H. Zhang, Q. Sun, R. Liu, J. Li, L. Wu, R. Tsao, Rapid and efficient conversion of all-*E*-astaxanthin to 9*Z*-and 13*Z*-isomers and assessment of their

stability and antioxidant activities. J. Agric. food Chem. 65 (2017) 818–826.

[40] Y. Yuan, Y. Gao, J. Zhao, L. Mao, Characterization and stability evaluation of β-carotene nanoemulsions prepared by high pressure homogenization under various emulsifying conditions. Food Res. Int. 41 (2008) 61−68.

[41] K.M. Koczkur, S. Mourdikoudis, L. Polavarapu, S.E. Skrabalak, Polyvinylpyrrolidone (PVP) in nanoparticle synthesis. Dalton Trans. 44 (2015) 17883−17905.

[42] S. Dong, Y. Huang, R. Zhang, Z. Lian, S. Wang, Y. Liu, Inclusion complexes of astaxanthin with hydroxypropyl-β-cyclodextrin: Parameters optimization, spectroscopic profiles, and properties. Eur. J. Lipid Sci. Technol. 116 (2014) 978−986.

[43] C. Yuan, Z. Jin, X. Xu, Inclusion complex of astaxanthin with hydroxypropyl-β-cyclodextrin: UV, FTIR, ^{1}H NMR and molecular modeling studies. Carbohydr. Polym. 89 (2012) 492−496.

[44] H.L. Hong, Q.L. Suo, L.M. Han, C.P. Li, Study on precipitation of astaxanthin in supercritical fluid. Powder Technol. 191 (2009) 294−298.

[45] V. Prosapio, I. De Marco, M. Scognamiglio, E. Reverchon, Folic acid-PVP nanostructured composite microparticles by supercritical antisolvent precipitation. Chem. Engi. J. 277 (2015) 286−294.

[46] İ.N., Uzun, O., Sipahigil, S., Dinçer, Coprecipitation of cefuroxime axetil–PVP composite microparticles by batch supercritical antisolvent process. J. Supercrit. Fluids 55 (2011) 1059−1069.

[47] J. Park, W. Cho, H. Kang, B.B.J. Lee, T.S. Kim, S.J. Hwang, Effect of operating parameters on PVP/tadalafil solid dispersions prepared using supercritical anti-solvent process. J. Supercrit. Fluids 90 (2014) 126−133.

[48] A. Gokhale, B. Khusid, R.N. Dave, R. Pfeffer, Effect of solvent strength and operating pressure on the formation of submicrometer polymer particles in supercritical microjets. J. Supercrit. Fluids 43 (2007) 341−356.

[49] M. Kalani, R. Yunus, Application of supercritical antisolvent method in drug encapsulation: a review. Int. J. Nanomed. 6 (2011) 1429−1442.

[50] J.I.N. Heyang, X.I.A. Fei, C. Jiang, Z.H.A.O. Yaping, H.E. Lin, Nanoencapsulation of lutein with hydroxypropylmethyl cellulose phthalate by supercritical antisolvent. Chin. J. Chem. Eng. 17 (2009) 672−677.

[51] A. Martin, F. Mattea, L. Gutierrez, F. Miguel, M.J. Cocero, Co-precipitation of carotenoids and bio-polymers with the supercritical anti-solvent process. J. Supercrit. Fluids 41 (2007) 138−147.

[52] J.S. Jin, C.W. Chang, J. Zhu, H. Wu, Z.T. Zhang, Solubility of poly (vinylpyrrolidone) with different molecular weights in supercritical carbon dioxide. J. Chem. Eng. Data 60 (2015) 3397−3403.

[53] H.S. Youn, M.K. Roh, A. Weber, G.T. Wilkinson, B.S. Chun, Solubility of astaxanthin in supercritical carbon dioxide. Kor. J. Chem. Eng. 24 (2007) 831−834.

[54] V. Prosapio, I. De Marco, E. Reverchon, PVP/corticosteroid microspheres produced by supercritical antisolvent coprecipitation. Chem. Eng. J. 292 (2016) 264−275.

[55] A.C. Boileau, N.R. Merchen, K. Wasson, C.A. Atkinson, J.W. Erdman, *Cis*-lycopene is more bioavailable than *trans*-lycopene in vitro and in vivo in lymph-cannulated ferrets. J. Nutr. 129 (1999) 1176−1181.

[56] N.Z. Unlu, T. Bohn, D.M. Francis, H.N. Nagaraja, S.K. Clinton, S.J. Schwartz, Lycopene from heat-induced *cis*-isomer-rich tomato sauce is more bioavailable than

from all-*trans*-rich tomato sauce in human subjects. Brit. J. Nutr. 98 (2007) 140−146.

[57] L. Müller, P. Goupy, K. Fröhlich, O. Dangles, C. Caris-Veyrat, V. Böhm, Comparative study on antioxidant activity of lycopene (*Z*)-isomers in different assays. J. Agric. food Chem. 59 (2011) 4504−4511.

Figure captions

Fig. 1. Chemical structures of (A) polyvinylpyrrolidone (PVP) and typical astaxanthin isomers: (B) (all-*E*)-astaxanthin; (C) (9*Z*)-astaxanthin; (D) (13*Z*)-astaxanthin.

Fig. 2. Schematic diagram of the SEDS process.

Fig. 3. SEM images of intact (A) PVP and (B) (all-*E*)-astaxanthin, and PVP/(all-*E*)-astaxanthin (20:1) coprecipitates obtained by SEDS process at temperature of 60 °C and pressures of 10 MPa.

Fig. 4. (A) Absorption spectra, (B) FT-IR spectra, and (C) XRD patterns of raw materials and PVP/(all-*E*)-astaxanthin (20:1) coprecipitates obtained by SEDS process at temperature of 60 °C and pressures of 10 MPa.

Fig. 5. Particle size distributions of PVP/(all-*E*)-astaxanthin (20:1) coprecipitates obtained by SEDS process (A) at temperature of 40 °C and various pressure, and (B) at pressures of 10 MPa and various temperature.

Fig. 6. Particle size distributions of (A) PVP/(all-*E*)-astaxanthin (various ratio) coprecipitates and (B) PVP/various *Z*-isomer content of astaxanthin (10:1) coprecipitates by SEDS process at temperature of 60 °C and pressures of 10 MPa.

Fig. 7. Reversed-phase HPLC chromatograms of (A) (all-*E*)-astaxanthin, (B) thermally treated astaxanthin at 80 °C for 8 h, and (C) the filtered astaxanthin. (9*Z*)- and (13*Z*)-Astaxanthin designated in the chromatograms were identified according to previous

studies [33,38,39].

Fig. 1

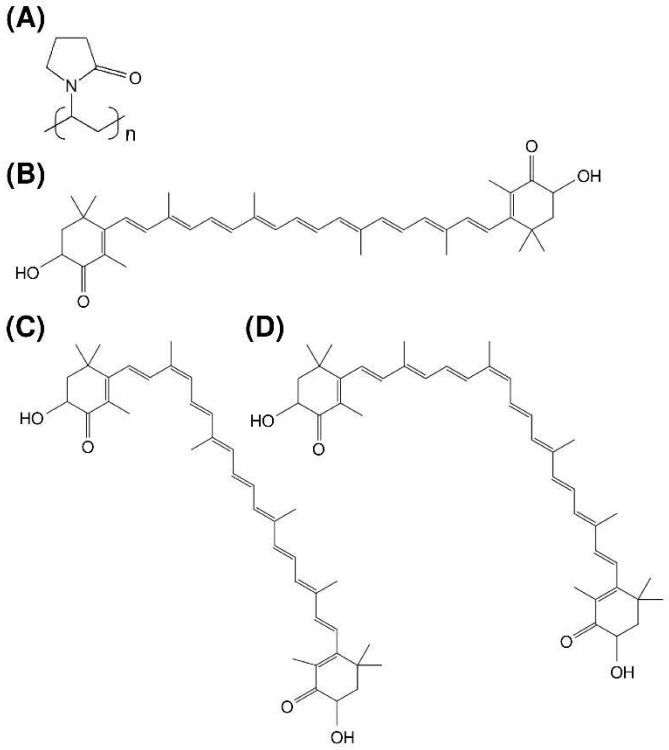

Fig. 2

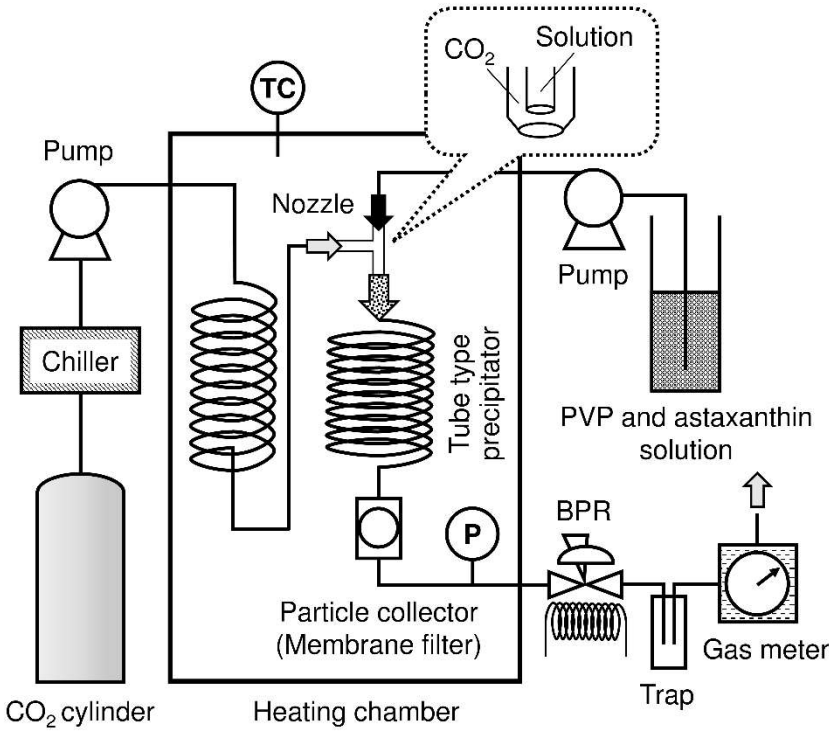
CO2
Solution
TC
Pump
Nozzle
Pump
Chiller
Tube type precipitator
PVP and astaxanthin solution
BPR
P
Particle collector (Membrane filter)
Gas meter
Trap
CO2 cylinder
Heating chamber

Fig. 3

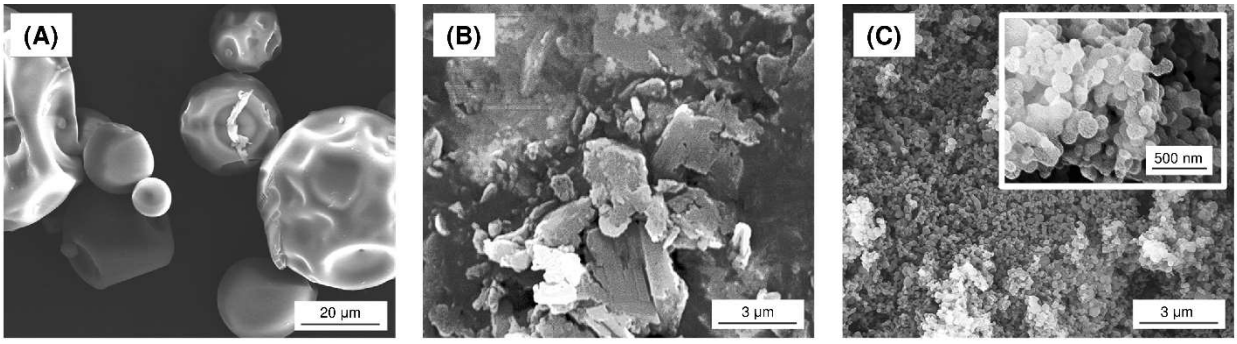

Fig. 4

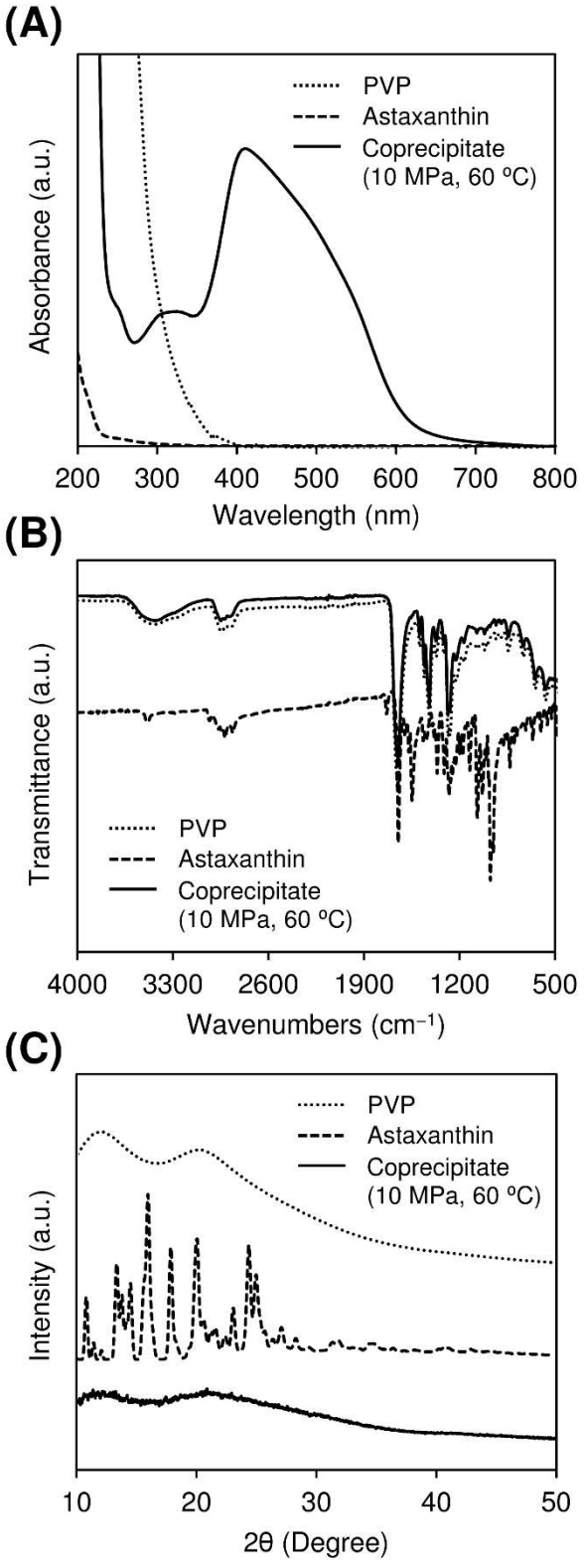
(A)
PVP
Astaxanthin
Coprecipitate
(10 MPa, 60 ºC)
Absorbance (a.u.)
200 300 400 500 600 700 800
Wavelength (nm)
(B)
Transmittance (a.u.)
PVP
Astaxanthin
Coprecipitate
(10 MPa, 60 ºC)
4000 3300 2600 1900 1200 500
Wavenumbers (cm⁻¹)
(C)
PVP
Astaxanthin
Coprecipitate
(10 MPa, 60 ºC)
Intensity (a.u.)
10 20 30 40 50
2θ (Degree)

Fig. 5

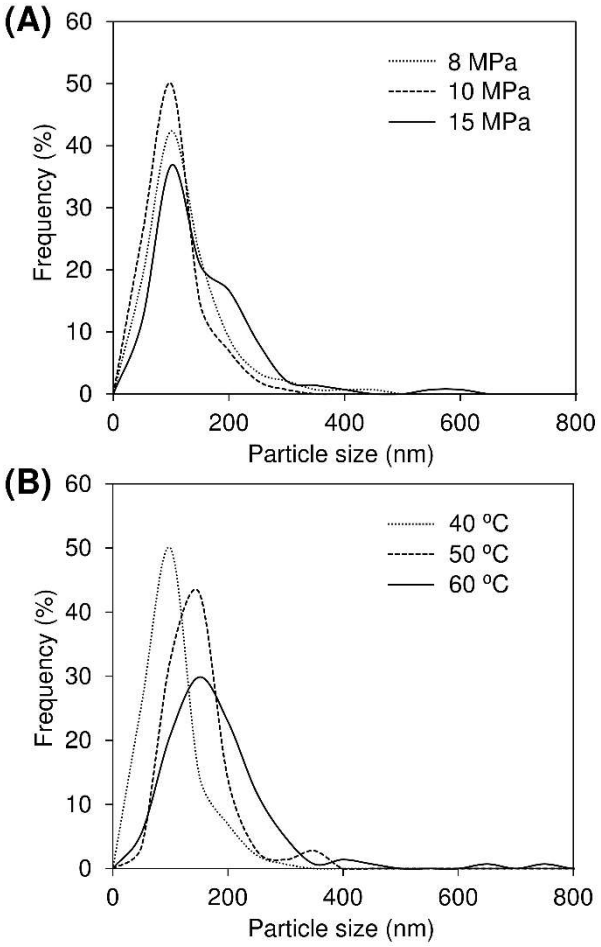
(A)
8 MPa
10 MPa
15 MPa
Frequency (%)
Particle size (nm)
(B)
40 ºC
50 ºC
60 ºC
Frequency (%)
Particle size (nm)

Fig. 6

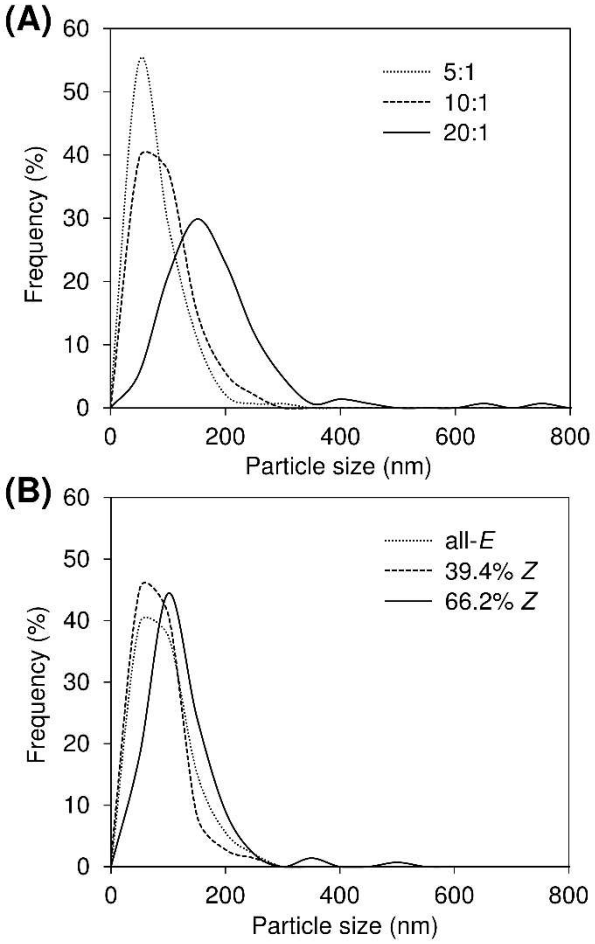
(A)
Frequency (%)
Particle size (nm)
5:1
10:1
20:1
(B)
Frequency (%)
Particle size (nm)
all-E
39.4% Z
66.2% Z

Fig. 7

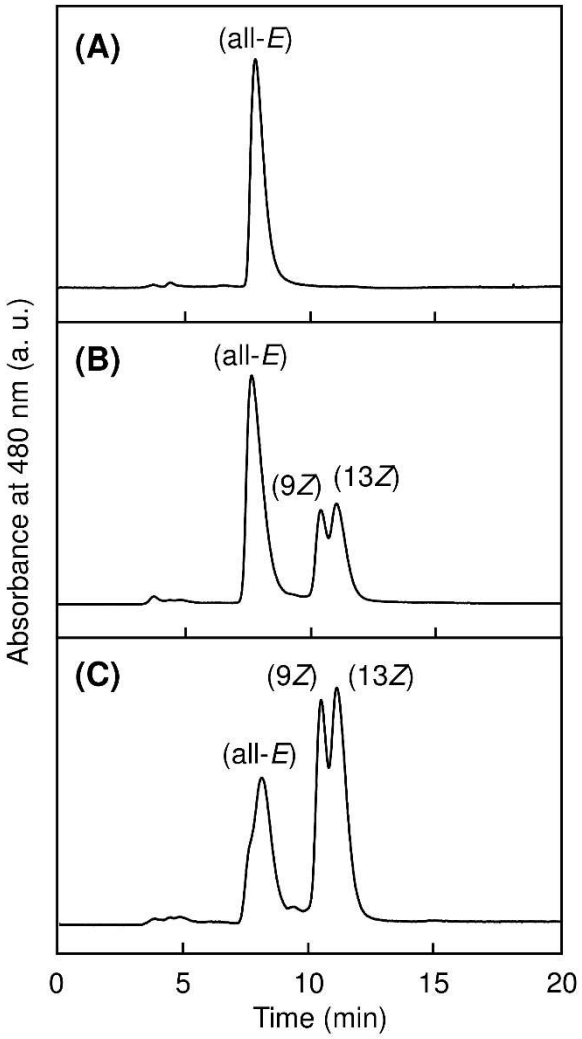
(A)
(all-E)
(B)
(all-E)
(9Z)
(13Z)
(C)
(9Z)
(13Z)
(all-E)
Absorbance at 480 nm (a. u.)
0
5
10
15
20
Time (min)

Table 1
Summery of SEDS experimental conditions.

No.	Pressure (MPa)	Temperature (°C)	PVP/astaxanthin ratio (w/w)[a]	*Z*-isomer content (%)[b]	Mean diameter (nm)	Astaxanthin content (%)[c]
1	8	40	20:1	−	152.7	0.51
2	10	40	20:1	−	132.6	0.33
3	15	40	20:1	−	175.0	0.07
4	10	50	20:1	−	174.4	0.49
5	10	60	20:1	−	203.1	1.43
6	10	60	10:1	−	124.8	3.91
7	10	60	5:1	−	99.1	3.90
8	10	60	10:1	39.4	105.6	3.78
9	10	60	10:1	66.2	141.7	3.56

[a] PVP and astaxanthin were dissolved in acetone/ethanol (19:1, v/v).
[b] Total *Z*-isomer content of astaxanthin. −, not detected substantially.
[c] Astaxanthin content in obtained PVP/astaxanthin coprecipitates by SEDS process.